CHALLENGES FACING THE GENERATION OF MW PROTON BEAMS USING RAPID CYCLING SYNCHROTRONS

Yoshiro Irie, JAERI/KEK
for the J-PARC Accelerator Group

What are challenging for RCS?

- Large aperture magnets and much higher RF voltages per turn due to a low energy injection and a large and rapid swing of the magnetic field,
- Field tracking between many magnet-families under slightly saturated conditions,
- RF trapping with fundamental and higher harmonic cavities,
- H^- charge stripping foil,
- Large acceptance injection/dump/extraction section,
- Ceramic chambers,
- Beam instabilities,
- Comparison with full-energy linac+storage ring approach from view point of the radiation protection.

These are discussed mainly on the basis of the J-PARC 3GeV RCS, which is under construction in Japan.

J-PARC LAYOUT

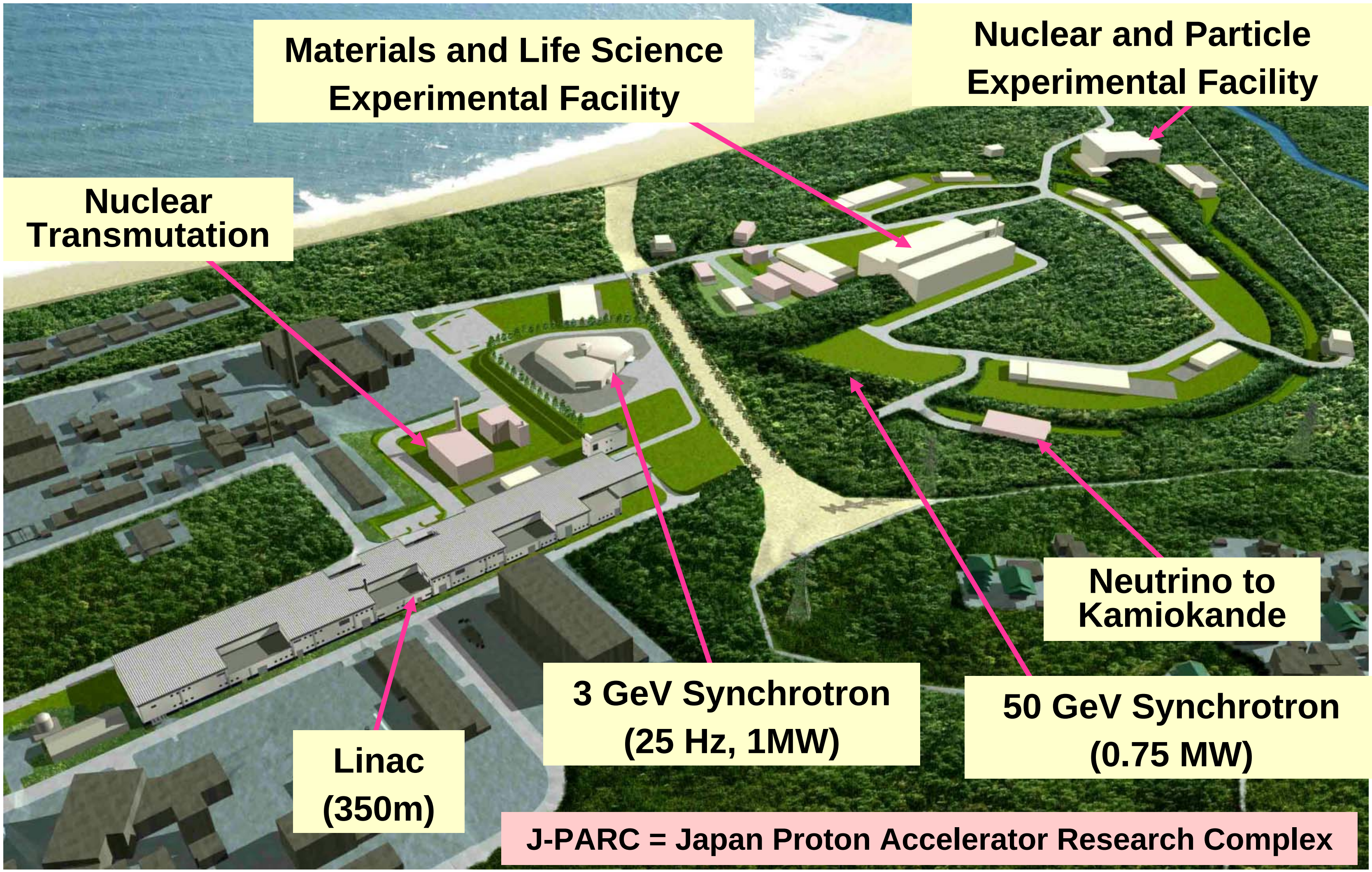

Phase 1 and Phase 2 (as of today)

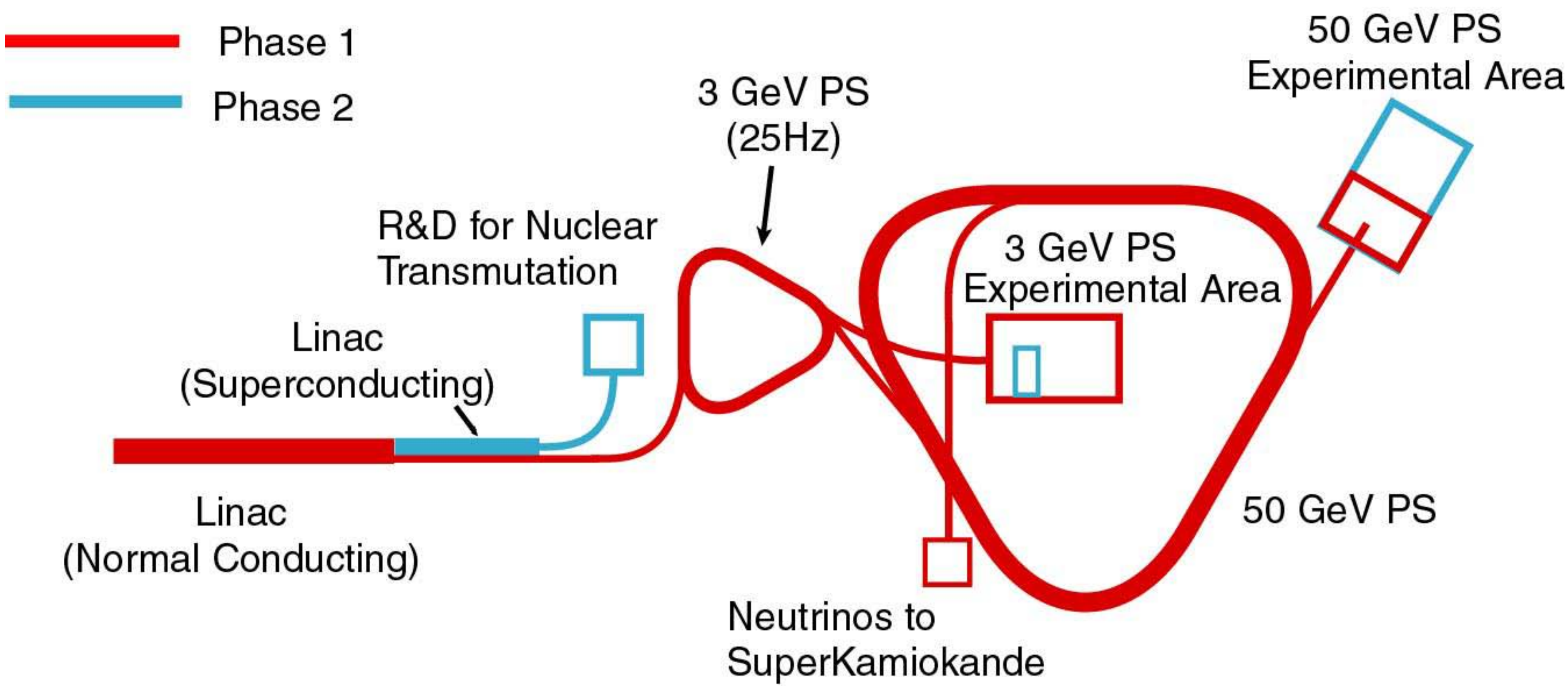

Aerial view of the J-PARC

RCS Building

RF section is under construction

Construction schedule

Construction Schedule

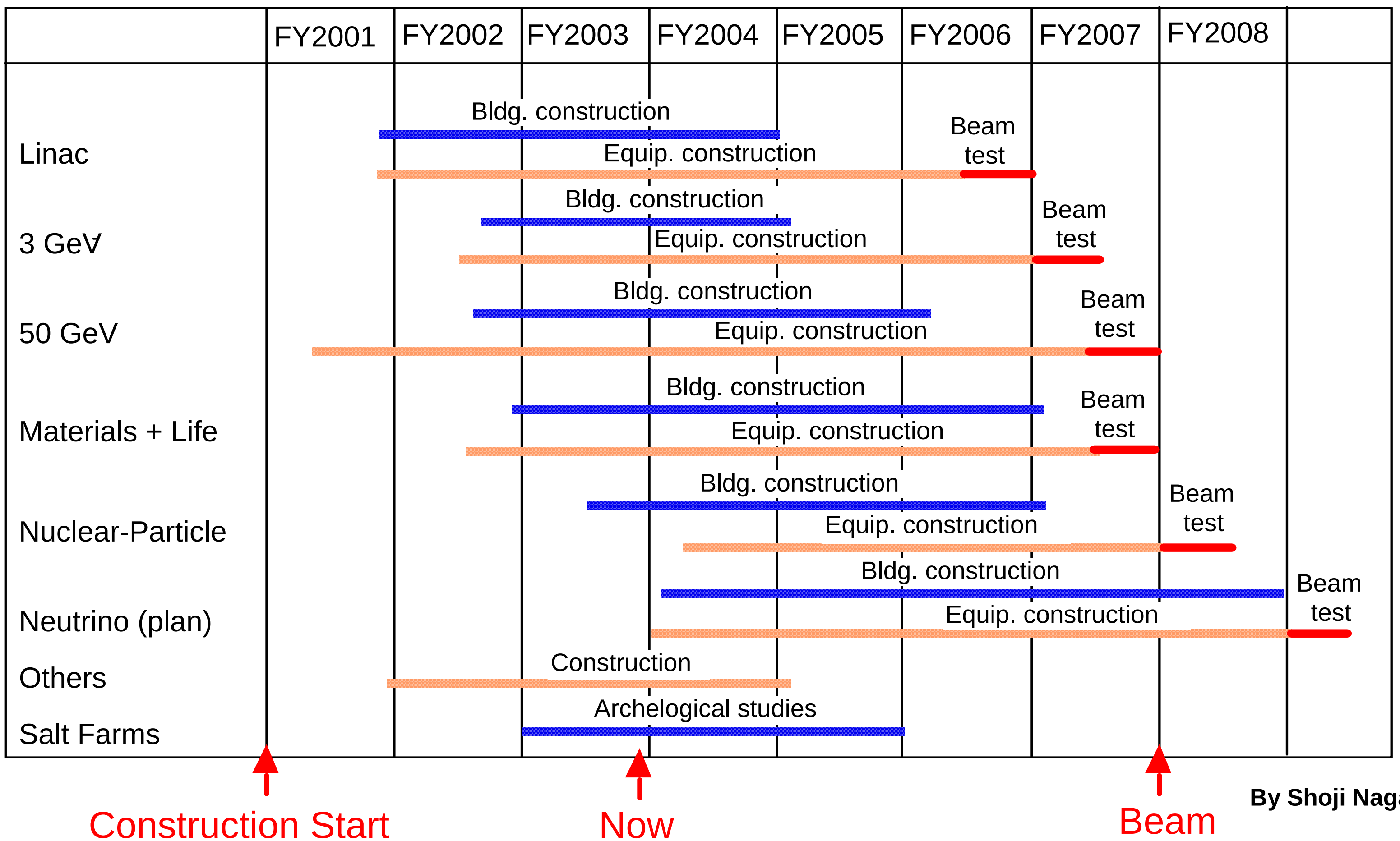

By Shoji Nagamiya

J-PARC 3GeV RCS Layout

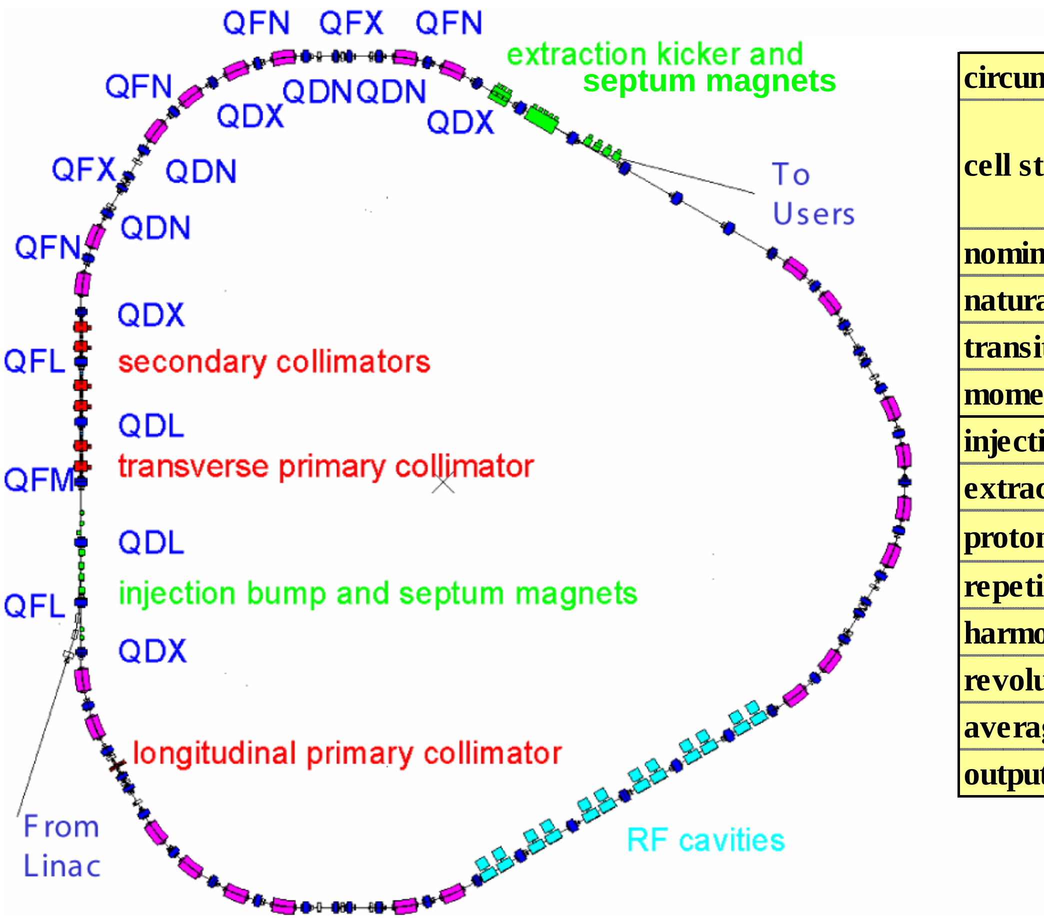

circumference	m	348.333
cell structure		(6 FODO arc + 3 FODO insertion) × 3
nominal tune	Q_x, Q_y	6.68, 6.27
natural chromaticity	ξ_x, ξ_y	-8.5, -8.8
transition gamma	γ	9.14
momentum compaction		0.012
injection energy	MeV	400
extraction energy	GeV	3
protons per pulse	10^{13}p	8.3
repetition rate	Hz	25
harmonics		2
revolution frequency	MHz	0.614~0.836
average output current	μA	333
output power	MW	1

H^- INJECTION

Horiz. view of the injection straight

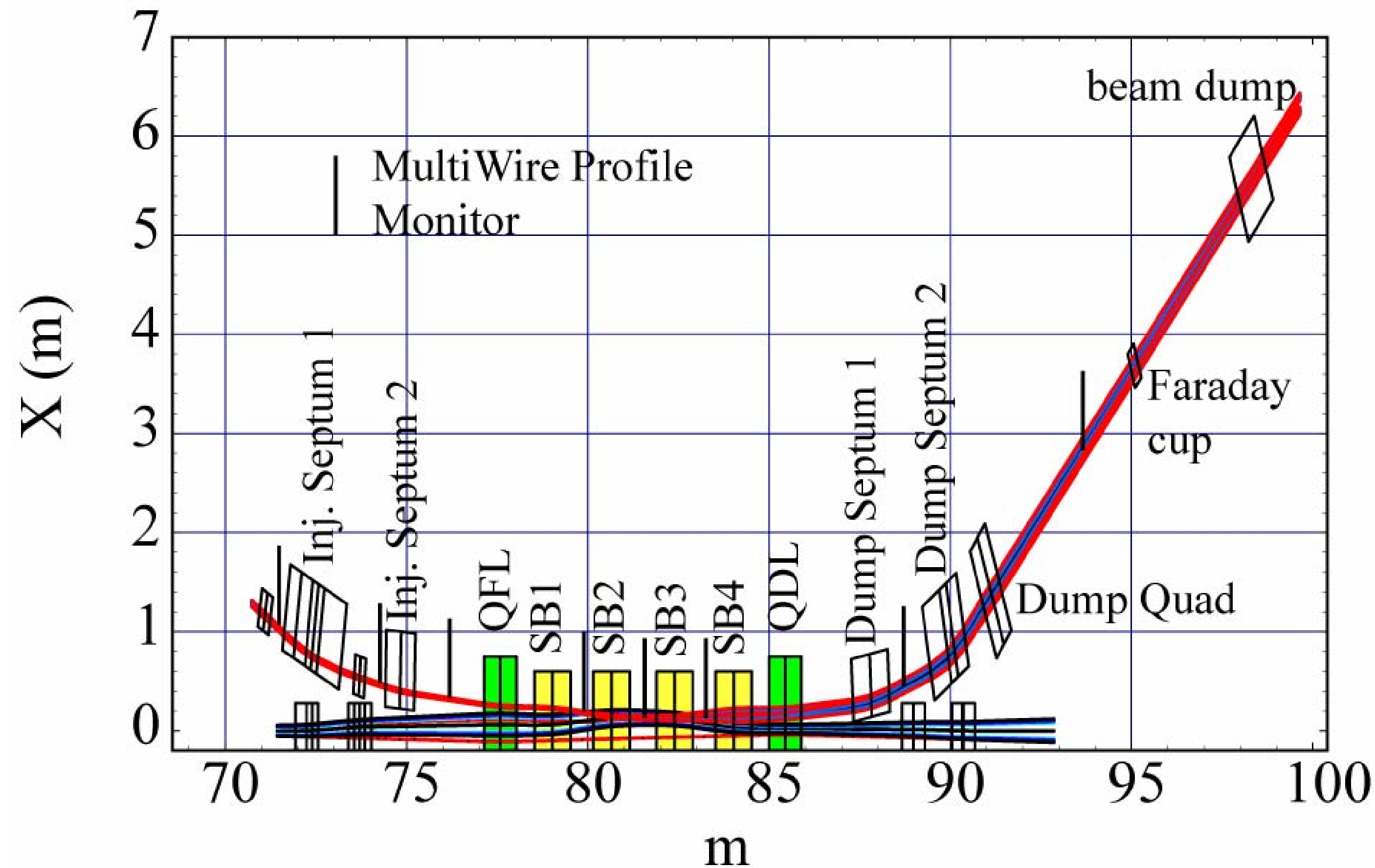

Magnet system comprises eight horizontal bump magnets and two vertical paint magnets. The vertical one is located π upstream of the foil location at the injection line, and the other one is used for correction when the phase advance is deviated from π. The horizontal bump magnets four shift-bump magnets (SB) which produces a fixed bump orbit, and four paint-bump magnets (PB).

H^- INJECTION

Horiz. details of the injection straight

H^- beam coming through non-linear field

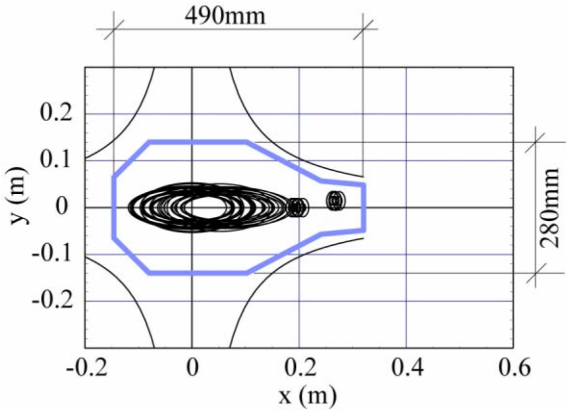

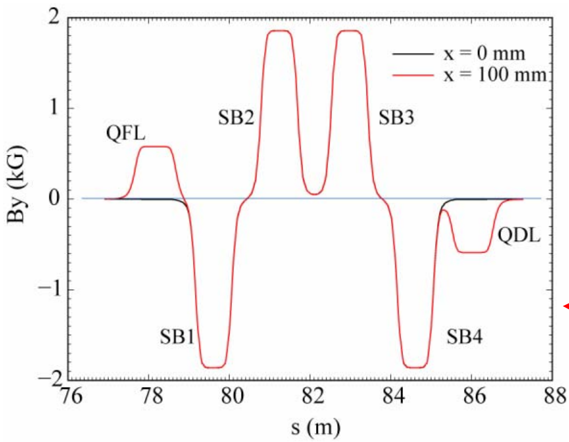

Optimize the field for electron collection (140W)

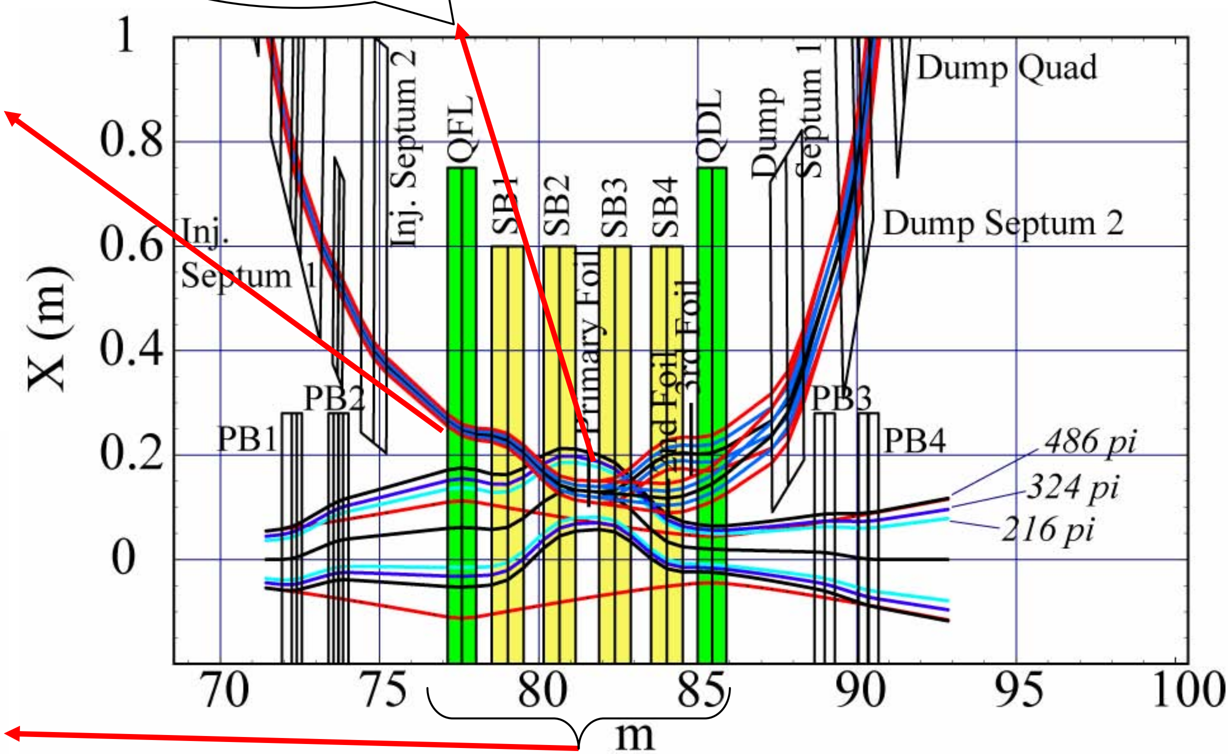

Field interference between large aperture magnets

H^- INJECTION

Vert. view of the injection straight

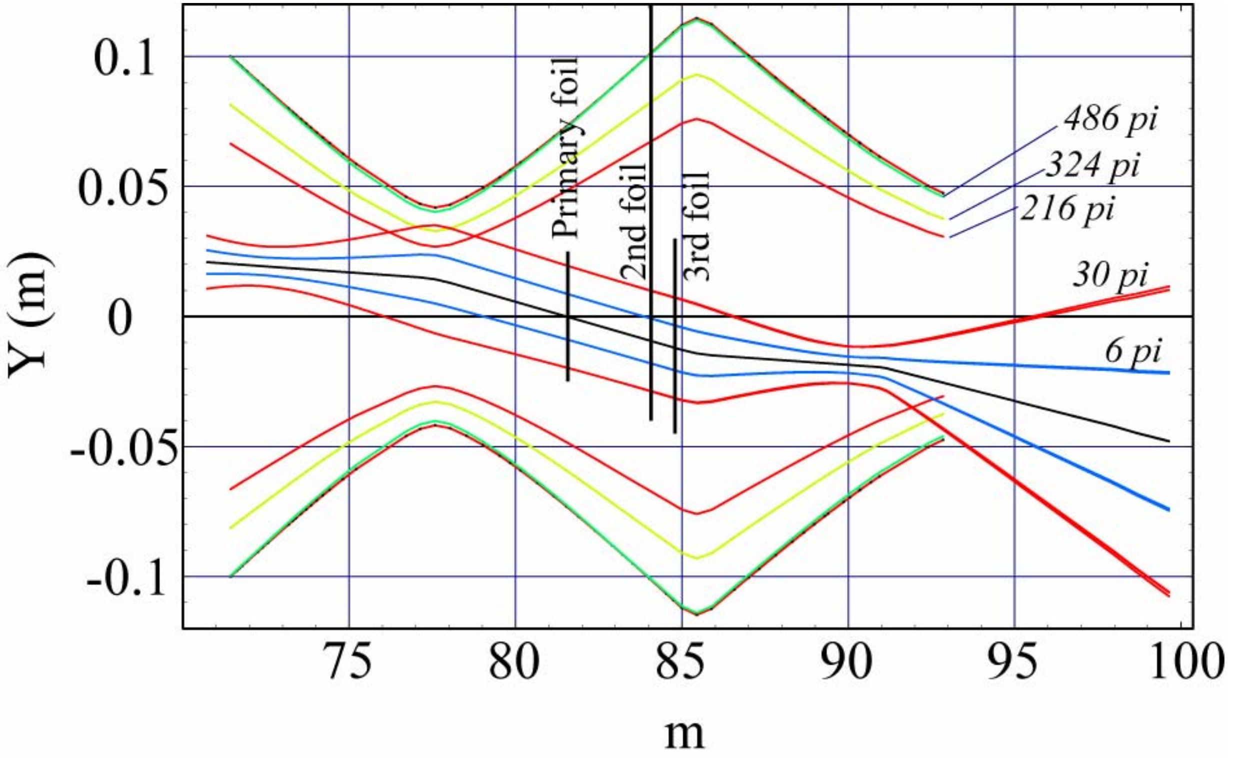

Three foils are used at the injection straight. 99.6% of the incoming H^- beam is converted into protons by the primary foil. The 2nd and 3rd are for H^0 and unstripped H^- beams. The shift-bump magnet is then split into two parts, and the 2nd foil is inserted in between.

H^- INJECTION

bump magnets

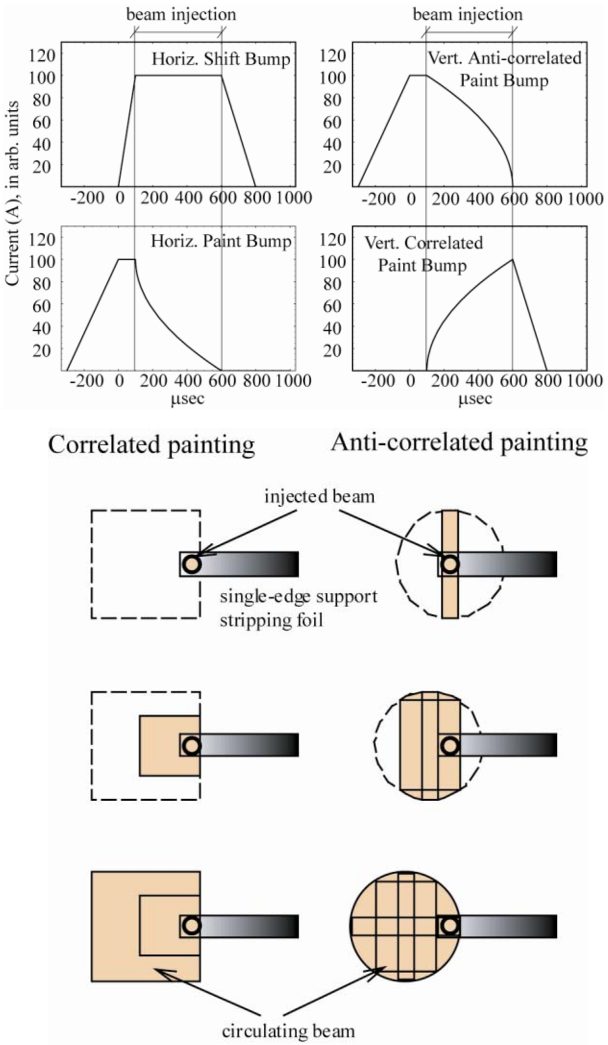

The bump system requires fast and flexible current pattern power supplies, which enable the correlated and anti-correlated paintings. The power supplies comprise rectifier and chopper sections, which utilize many high power IGBT's (Insulated Gate Bipolar Transistor) in series and/or parallel to realize the high power operation with a tracking error less than 1%.

Specifications for the bump power supply.

Tracking error is 1%.

Power supply	No.	Voltage (KV)	Current (KA)	IGBT rating	effective carrier frequency (KHz)
Horiz. SB	1	10.0	32.2	3300V, 1200A	60
Horiz. PB	4	1.2	29.0	1200V, 300A	1800
Vert. PB	2	0.6	3.4	1200V, 300A	1800

H^- INJECTION

bump magnet power supply

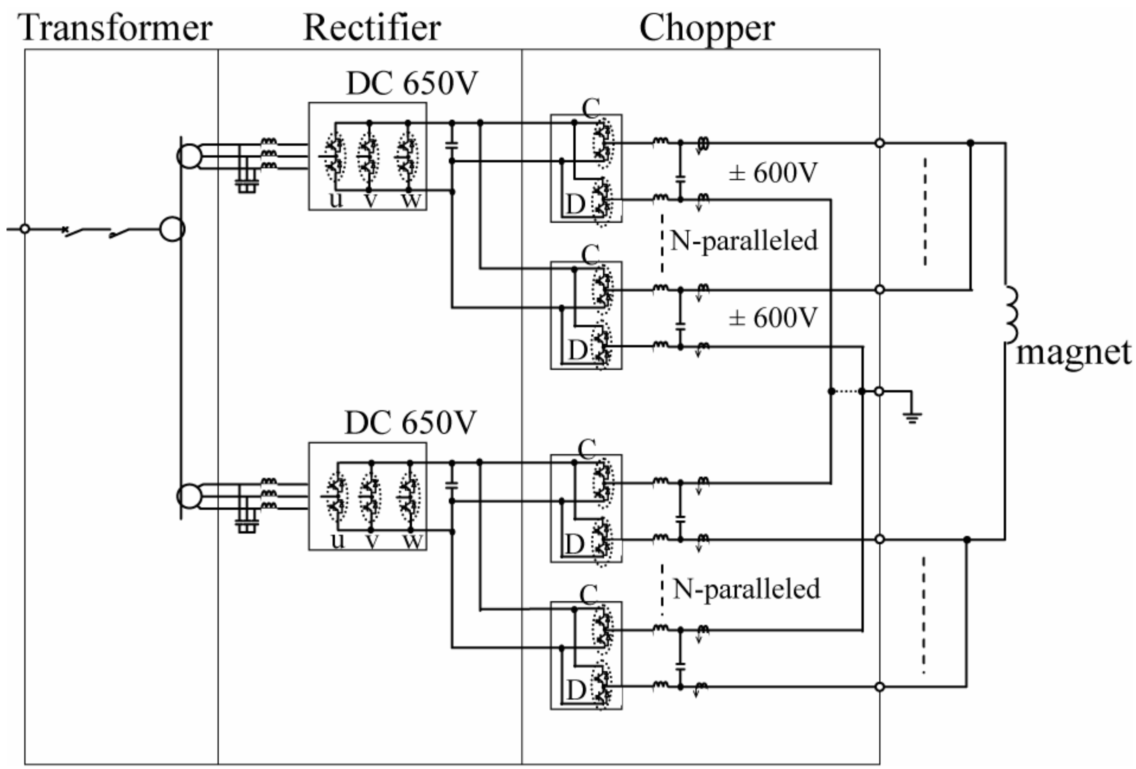

Power supply for a paint bump magnet.

H^- INJECTION

H- stripping foil

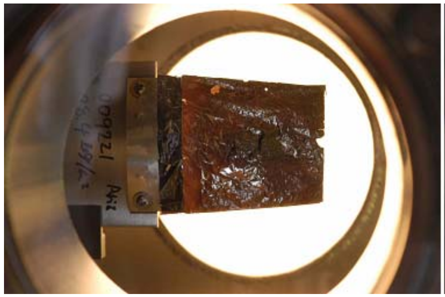

used for 3days

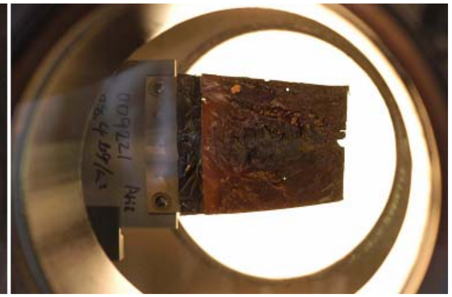

10days

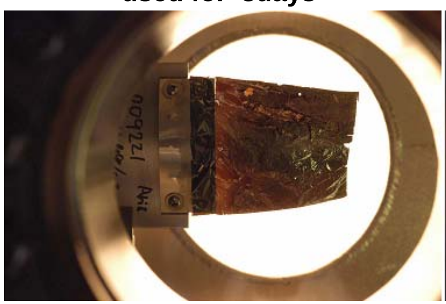

17days

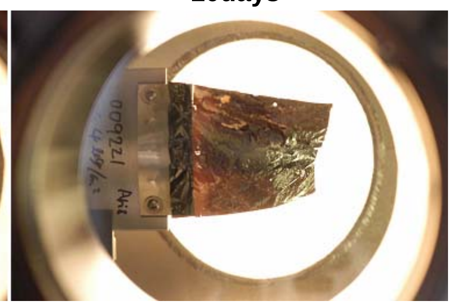

24days

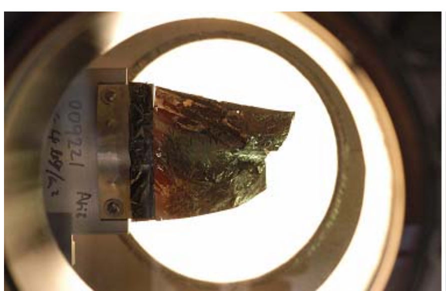

31days

38days

Photo: KEK booster H^- foil

Very difficult part of the RCS:

- **Foil degradations by the beam will be serious.**
- **In the KEK booster synchrotron, a single-edge-support carbon foil of 60μg/cm^2 is used (see left). Energy deposition ~0.73W/area.**
- **At the J-PARC RCS, energy deposition ~5.8W/area !**
- **Temperature rise is upto ~1,500K with emissivity=0.2.**

Extraction

aperture

- Thanks to the adiabatic damping, the beam, which will extend over the collimator aperture at the initial stage of acceleration, may damp according to,

$$(\beta\gamma)_{0.4GeV} / (\beta\gamma)_{3GeV} \sim 0.25.$$

- Aperture of the extraction channel is designed to be the same with the collimator aperture (324π) in the ring for low loss operations.

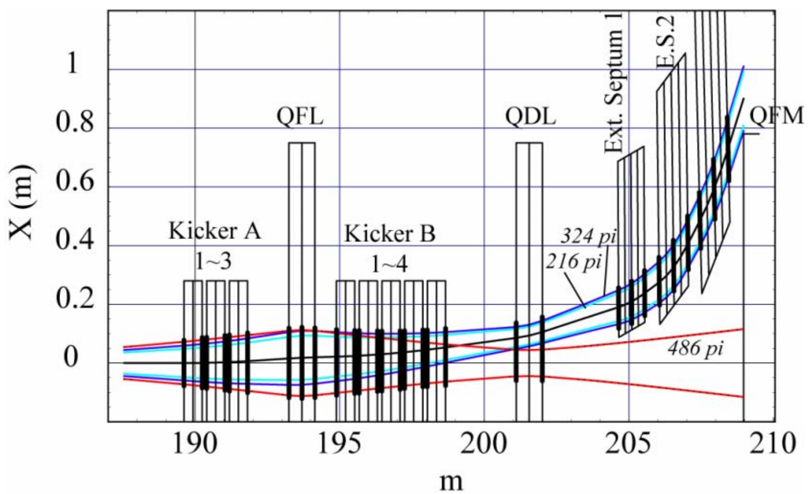

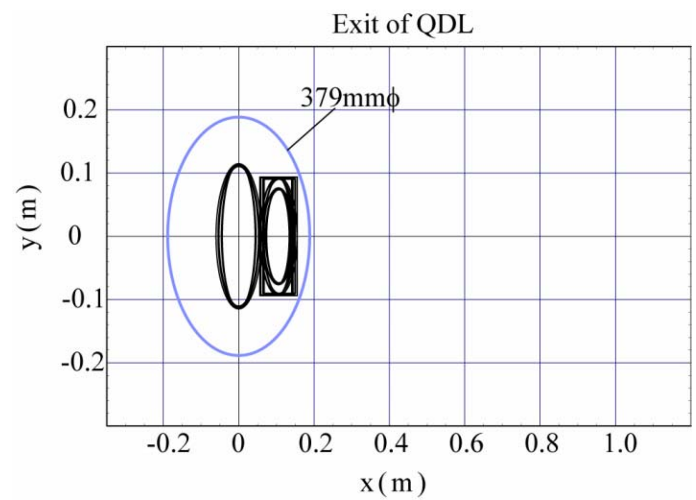

Extraction

Kicker magnet

Gap height : 160 mm, Gap width : 280 mm, Charging voltage : 60kV, Impedance : 10ohm, Current : 4,000A, Pulse width : 1.3 μs, rise time for power supply : < 100ns

Test of thyratron switch is in progress at 80KV.

RF

high gradient cavity

Higher RF voltage gain is a remarkable aspect of the RCS, where the peak RF voltage per turn is 450KV. A high gradient cavity has been developed at KEK for this purpose, which is capable of producing more than twice as much of the conventional ferrite loaded cavity. High power test on the cut core of the magnetic alloy is in progress.

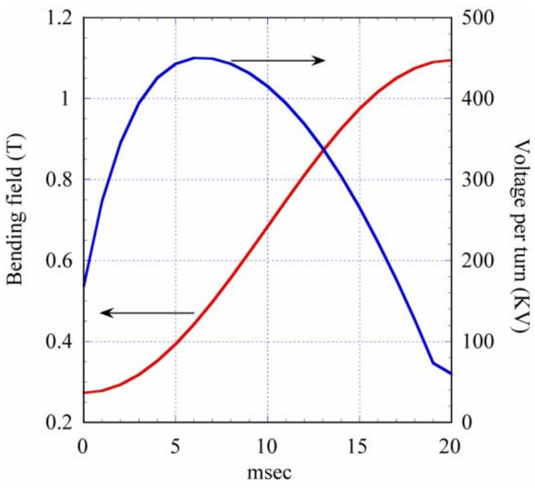

Sinusoidal guide field (red) and the required RF voltage (blue). Bucket area has twice as much as the beam emittance, 3.5eV•sec.

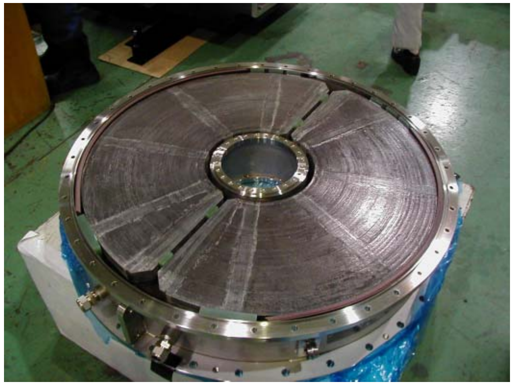

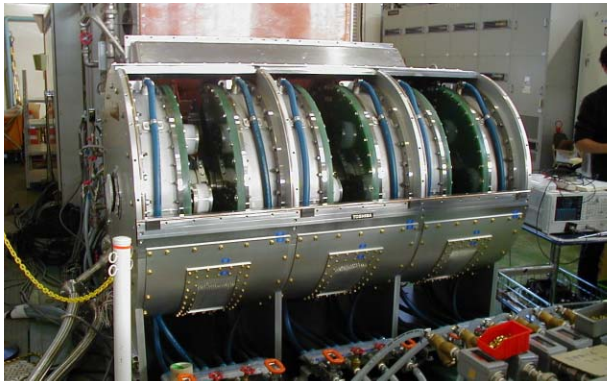

MA cut core (left) and the MA loaded cavity (right).

RF parameters

Number of cavities		11
Length of cavity	m	2
Voltage per cavity	KV	45
Number of gaps per cavity		3
Number of MA cores per cavity		18
Unloaded Q value		~2
Impedance per gap	Ω	~840
Impedance per cavity (seen by the beam)	Ω	~1,800
Resonant frequency	MHz	~1.5
Operating frequency	MHz	0.9~5.1
Beam loading		
circulating current	A	8.2~11.1
fundamental component	A	10~21
second harmonic	A	< 18
third harmonic	A	< 13
RF amplifier		TH558×2 in push-pull mode
Anode power supply		
output voltage	KV	10
output current	A	120

RF

precise control and beam loading (1)

- Second harmonic component is superimposed on the same cavity to improve the bunching factor.

$$V_{rf} = V_1 \sin\phi + V_2 \sin 2(\phi - \phi_s + \phi_2),$$
$$V_2 = 0.8\,V_1 \cos\phi_s,$$

- Phase error of 5 degrees will cause the difference of the bunching factor by ~0.05.

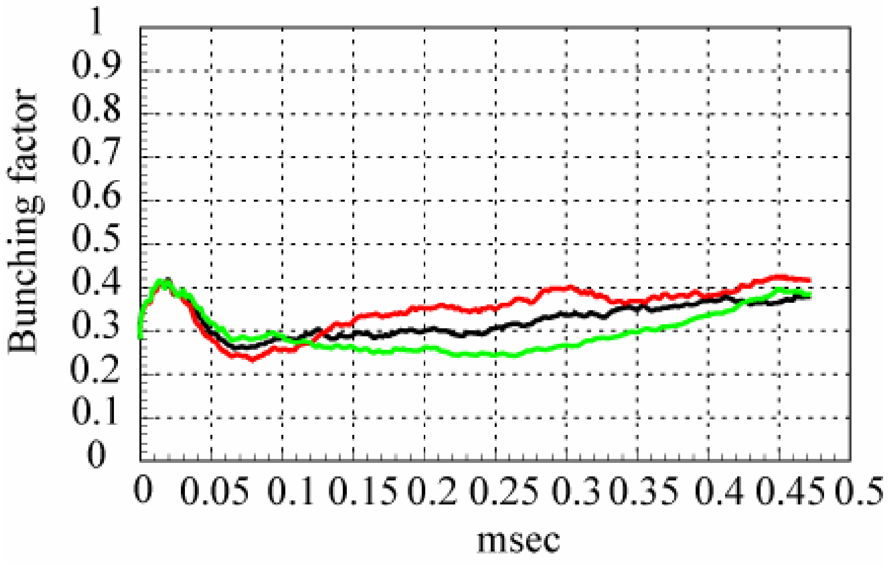

Variations of bunching factor during injection.

Initial phase of the second harmonic cavity to the fundamental one is 25deg. (black), 30deg. (red) and 20deg. (green)

RF
precise control and beam loading (2)

- Fundamental component reaches 10A after the injection end, giving relative loading Y~1.2.
- Beam loading cancellations including higher harmonics are essential for the precise control of the system. The beam feedforward system will be applied upto 3rd harmonics (h=6).
- Feasibility study of the low-output-impedance approach for the beam loading cancellation is in progress by the collaboration between ANL/ISIS/KEK/JAERI.

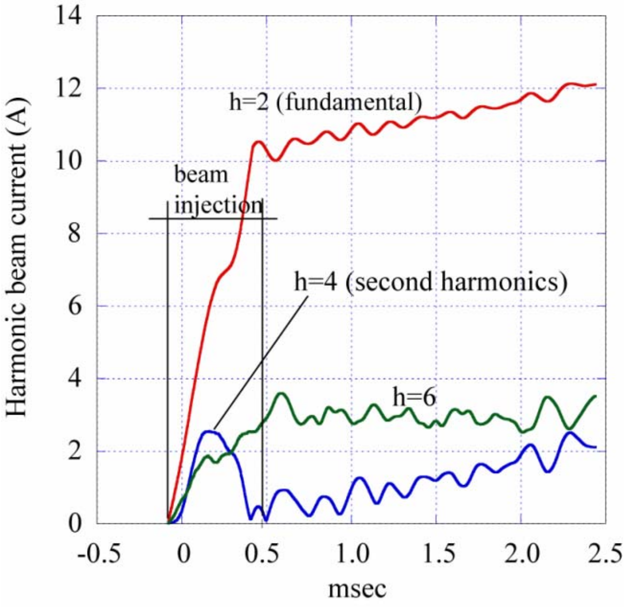

Harmonic contents in the trapping and early stage of acceleration

MAGNET

BM+7 quad families

In order to cover a wider range of the RCS operation tunes, the quadrupole magnets have been grouped into seven families with different dimensions.

Parameter	Units	BM	QM (A-type)	QM (B-type)	QM (C-type)	QM (D-type)
Family name			QFN,QDN,QDX	QFM	QFX	QFL, QDL
Number of magnets		24+1	33	3	12	12
Minimum field	T, T/m	0.27	0.67	0.47	0.65	0.47
Maximum field	T, T/m	1.10	4.84	3.37	4.67	3.36
Gap distance or Bore diameter	mm	210	290	330	330	410
Core length	mm	2770	700	900	500	900
Turns per coil	turn	36	31	31	31	31
Size of stranded coil conductor	mm^2	30×30	20×20	20×20	20×20	20×20
DC current	A	1566.6	747	672.4	934	1033.7
AC current	A	1170.9	565.3	507.5	706	784.7
Field quality	$\Delta B/B$, $\Delta B'/B'$	$<5\times10^{-4}$	$<5\times10^{-4}$	$<5\times10^{-4}$	$<5\times10^{-4}$	$<5\times10^{-4}$
Good field region	mm	±120	±124.5	±142.5	±142.5	±120
Resistance	mΩ	31.5	42.2	48.6	35.9	48.9
Inductance	mH	66	42.8	44.9	28.1	39.1

MAGNET

photos

Bending magnet

Quadrupole magnet

MAGNET

power supplies

- Power supply of the bending magnets is divided into ac and dc supplies, which comprise the White circuit, since the excitation current is much higher than those of the quadrupole magnets (fig.a).
- All the quad magnets within a family are connected in series to the power supply, and are fed by the dc-biased sinusoidal ac current (fig.b).

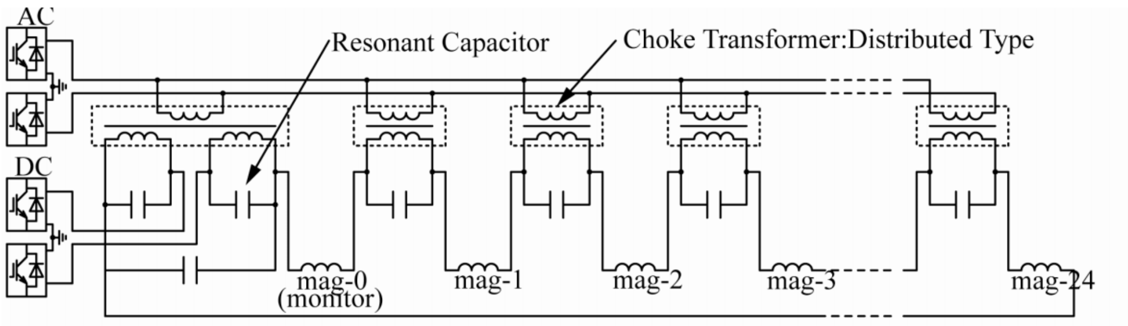

(a)Bending magnet Power supply

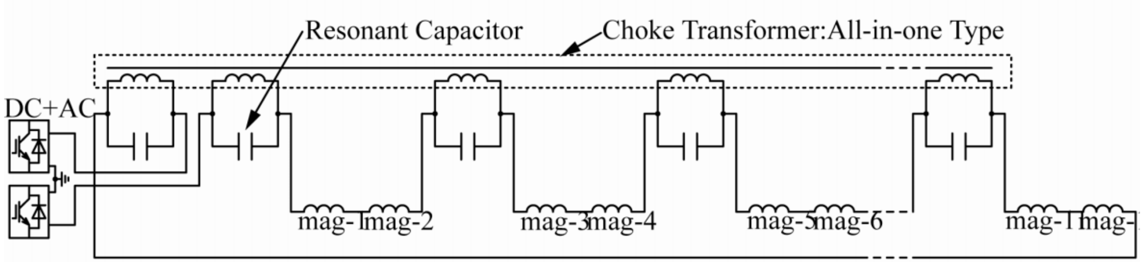

(b)Quadrupole magnet Power supply

MAGNET

field saturation (1)

Field saturation of the dipole magnet has been observed by the field calculations.

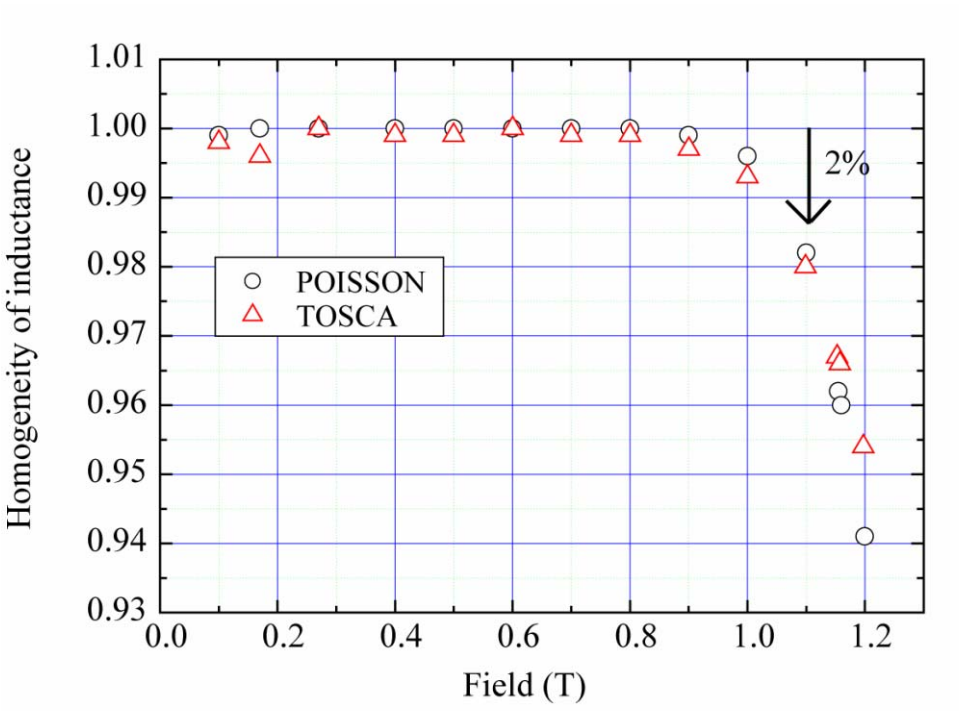

Field saturation of the dipole magnet. Horizontal axis shows the ideal field produced by a given coil current.

MAGNET

field saturation (2)

Tracking error of the quadrupole magnets to the dipole magnet field can be calculated as, assuming the quad field is ideal,

$$\frac{\Delta K}{K} = \frac{1 - \alpha\cos\omega t}{1 + \frac{a_2}{B_{dc}} - \alpha\cos\omega t(1 - 3\frac{a_3}{a_1} + 2\frac{a_2}{a_1}\cos\omega t + 4\frac{a_3}{a_1}\cos^2\omega t)} - 1,$$

where $\alpha = B_{ac}/B_{dc} = 0.6$ and the saturated ac field is expressed as,

$$B_{ac}(t) = a_1\cos\omega t + a_2\cos 2\omega t + a_3\cos 3\omega.$$

with a_1=0.44411, a_2=0.0024 and a_3=0.001392.

MAGNET

field saturation (3)

- Tracking error reaches its maximum of 1.3% at injection without any harmonic corrections. Tune shift caused by this error is estimated to be 0.12.
- Correction of the field distortions is essential.
- Locations of the trim quads have been assigned.

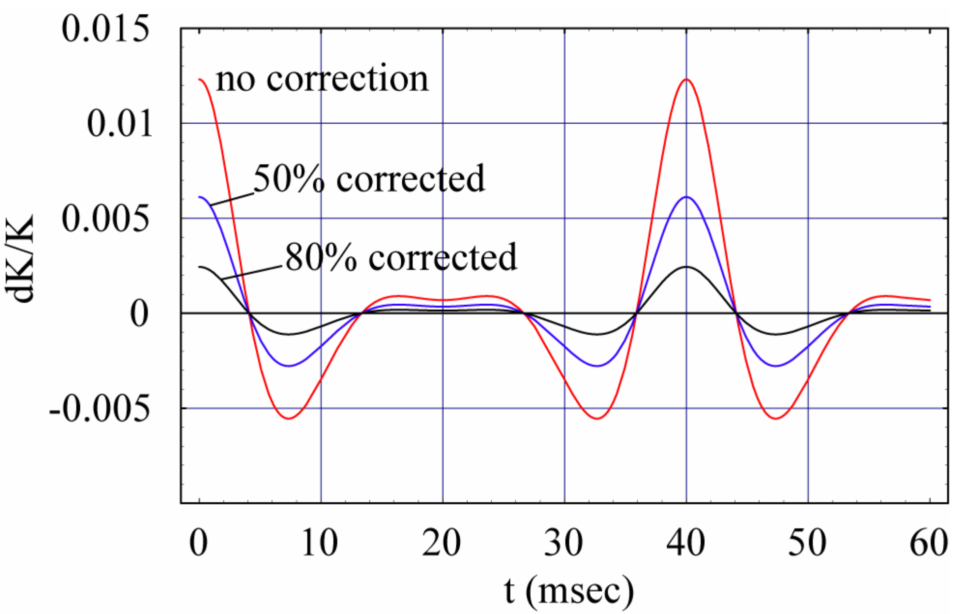

Ceramics Vacuum Chamber

The ceramic vacuum chambers are used at the ac and pulsed magnet sections in order to avoid an excessive heating by the alternating magnetic field.

- Chamber Joint
  with metalizing & brazing

- RF Shield
  copper with electrotyping methods

D:260 mm, L:1,200 mm, rf shield:100 lines

- TiN Coating at inside
  to suppress secondary emission

- Ti Flange
  for lower activation

Ceramics Vacuum Chamber R&D

- Deformations of the ceramic during sintering in a furnace: For a 1m-long chamber with a circular cross section (200mmϕ, 7.5mm thick), circularity and straightness are both less than 1mm without grinding or polishing process.
- However, a chamber with a pear-like cross section at the injection straight quadrupole needs R&D on the deformations.

Ceramic chamber at the injection straight quadrupole(QFL).

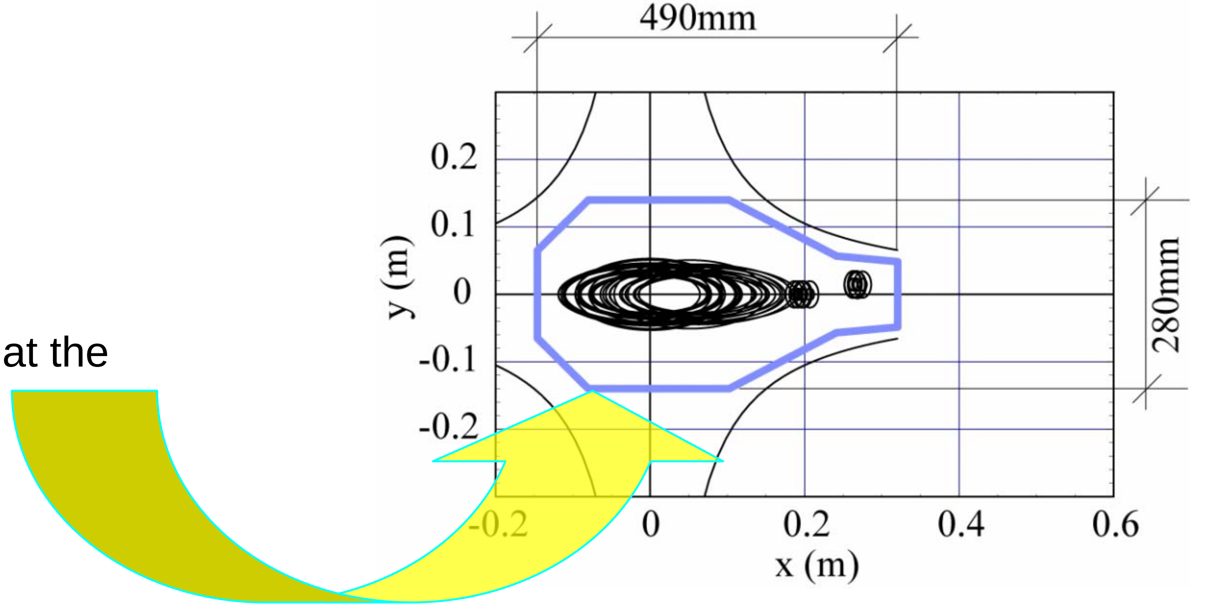

Electron-Proton Instability

- Electron-proton instability is thought to be strong and fast instability for the high intensity machine.
- Many reports have been published on the instability. There is no report, however, to explain why such instability is observed at PSR, and not in ISIS, by taking into account the real primary electrons produced.
- Electron cloud is formed by the trailing-edge multipacting process, and strongly depends upon the parameters such as primary electron production rate, secondary electron yield, beam size, chamber size, bunch length and bunch spacing.

Electron-Proton Instability

K.Ohmi ('03) has calculated the threshold neutralization, assuming the primary electron production rate

$Y1=4.4\times10^{-6}e/(\text{meter}\bullet\text{proton})$, and the secondary yield $Y2,max=2.1$.

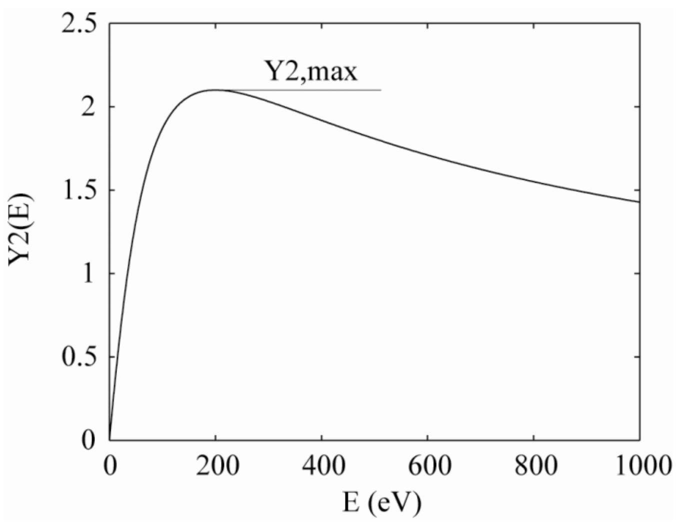

Secondary electron yield vs primary electron energy.

Electron-Proton Instability

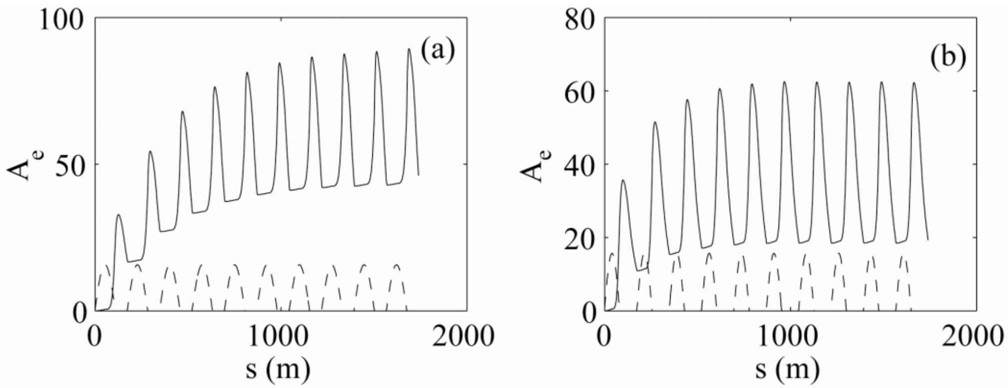

Amplification factor (Ae) for the 3GeV RCS at (a) injection and (b) extraction,

Ae= (number of created electrons) /(number of primary electrons)

neutralization	3GeV RCS		PSR	ISIS	SNS
	injection	extraction			
f(bottom)	0.020	0.007	0.034	0.003	0.007
f(peak)	0.042	0.023	0.067	0.005	0.250
f(threshold)	0.280	0.030	0.021	0.417	0.063

Results of simulations:

3GeV RCS ($4.15x10^{13}$p/bunch) and ISIS ($1.25x10^{13}$p/bunch) are safe, and not in PSR ($3.0x10^{13}$p/bunch) and SNS ($20.5x10^{13}$p/bunch) .

Electron-Proton Instability

- These results are, however, drastically changed if different assumptions are adopted. For example, taking $Y_{2,max}=1.5$ which is the case for TiN coated surface, the neutralizations at the peak and bottom become 0.006 and 0.0038, respectively at the PSR, which are now well below the threshold value of 0.021.
- Also, it should be required to identify the proton loss rate in the actual machines: for example, primary electrons coming from the stripping process at the foil, $Y_1 \sim 2.0\times10^{-5}$ e/(meter•proton) for 3GeV injection, is neglected in the present calculations.
- It is prudent to have provisions of TiN coating and a weak solenoid in the ring to suppress the multipacting.

Radiation protection

Given proton losses in KW, the residual radioactivity and absorbed dose at the beam collimator region were compared for the variety of injection energies by means of the MARS code. The total loss of protons in the ring was assumed to be 3.6KW for all cases, and the collimator section in the old JHF 3GeV ring was used for model calculations.

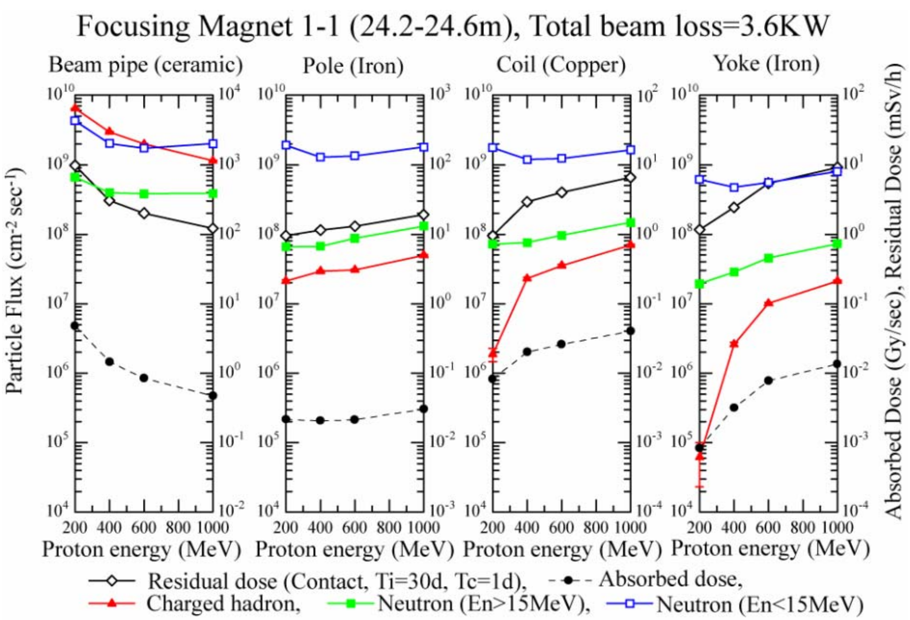

Result of MARS calculations for a quadrupole magnet next to the primary collimator.

Residual and absorbed dose rates increase with the injection energy.

Summary

- Challenging aspects to generate the MW beams using RCS are surveyed.
- H^- injection/extraction sections are very congested: final arrangements and specifications of the modules are in progress.
- Comaprison with full-energy linac+storage ring is made from view point of radiation protection.
- First beam commissioning of the J-PARC 3GeV RCS is scheduled in early FY 2007.